NACA TN 2595

NATIONAL ADVISORY COMMITTEE FOR AERONAUTICS

TECHNICAL NOTE 2595

DESIGN OF TWO-DIMENSIONAL CHANNELS WITH PRESCRIBED VELOCITY DISTRIBUTIONS ALONG THE CHANNEL WALLS

II - SOLUTION BY GREEN'S FUNCTION

By John D. Stanitz

Lewis Flight Propulsion Laboratory
Cleveland, Ohio

Washington
January 1952

.L

NATIONAL ADVISORY COMMITTEE FOR AERONAUTICS

TECHNICAL NOTE 2595

DESIGN OF TWO-DIMENSIONAL CHANNELS WITH PRESCRIBED VELOCITY DISTRIBUTIONS ALONG THE CHANNEL WALLS

II - SOLUTION BY GREEN'S FUNCTION

By John D. Stanitz

2390

SUMMARY

Methods of solution by Green's function are developed for the design of two-dimensional unbranched channels with prescribed velocities as a function of arc length along the channel walls. The methods apply to incompressible and linearized compressible, nonviscous irrotational flow. One numerical example is presented for an accelerating elbow with linearized compressible flow. The elbow shape obtained from the solution by Green's function is the same as that obtained from a solution by relaxation methods for the same prescribed conditions. The time required for the calculations is considerably less for solutions by Green's function.

INTRODUCTION

In this report a general method of design is developed for two-dimensional, compressible or incompressible, nonviscous irrotational flow in unbranched channels with prescribed velocities as a function of arc length along the channel walls. The design of channels with prescribed velocities is important because: (1) boundary-layer separation losses can be avoided by prescribed velocities that do not decelerate rapidly enough to cause separation, (2) shock losses in compressible flow and cavitation in incompressible flow can be avoided by prescribed velocities that do not exceed certain maximum values dictated by these phenomena, and (3) for compressible flow the desired flow rate can be assured by prescribed velocities that do not result in "choke flow" conditions.

In Part I of this report (reference 1) solutions were obtained by relaxation methods. This method of solution results in complete information concerning the distribution of flow conditions throughout the channel and can be used to obtain solutions for incompressible flow and for two types of compressible flow: the general type with arbitrary value for the ratio of specific heats γ (1.4, for example) and the linearized type with γ equal to -1.0.

In the present report solutions are obtained by Green's function. This method of solution is limited to incompressible and linearized ($\gamma = -1.0$) compressible flow, but the method is more rapid than relaxation methods, provided information within the channel is not required. The method of solution is developed for the channel walls only although the method can be extended to determine the shape of streamlines within the channel.

The design method reported herein was developed at the NACA Lewis laboratory during 1950 and is part of a doctoral thesis conducted with the advice of Professor Ascher H. Shapiro of the Massachusetts Institute of Technology.

METHOD OF SOLUTION

The design method is developed for two-dimensional channels with prescribed velocities along the channel walls. The prescribed velocity is arbitrary except that stagnation points (zero velocity) cannot be prescribed. This exception limits the design method to unbranched channels. In the present report the method of solution is by Green's function in conjunction with a formula derived (elsewhere) from Green's theorem.

Preliminary Considerations

Assumptions. - The fluid is assumed to be nonviscous and either compressible or incompressible. If the fluid is compressible, the ratio of specific heats γ is assumed to be -1.0, so that the differential equations describing the flow are linear. The flow is assumed to be two-dimensional and irrotational.

Physical plane. - The flow field of the two-dimensional channel is considered to lie in the physical xy-plane where x and y are Cartesian coordinates expressed as ratios of a characteristic length equal to the constant channel width downstream at infinity. (All symbols are defined in appendix A.)

At each point in the channel the velocity vector (fig. 1) has a magnitude Q and a direction θ where Q is the fluid velocity expressed as the ratio of a characteristic velocity equal to the constant channel velocity downstream at infinity. For compressible flow, the velocity Q is related to the velocity q by

$$q = Qq_d \tag{1}$$

where q is the velocity expressed as a ratio of the stagnation speed of sound and the subscript d refers to conditions downstream at infinity.

Stream function Ψ. - If the condition of continuity is satisfied, a stream function Ψ can be defined such that for incompressible flow

$$d\Psi = \frac{\pi}{2}\, d\psi \tag{2a}$$

where, from Part I,

$$d\psi = Q\ dn \tag{2b}$$

where n is distance in the xy-plane measured normal to the streamline and expressed as a ratio of the channel width downstream at infinity. For linearized compressible flow $(\gamma = -1.0)$

$$d\Psi = \frac{\pi}{2}\,\frac{d\psi^*}{\Delta\psi^*} \tag{2c}$$

where, from Part I,

$$d\psi^* = \rho^* q^*\ dn \tag{2d}$$

and where $\Delta\psi^*$ is the value of ψ^* along the left channel wall when faced in the direction of flow if the value of ψ^* along the right wall is arbitrarily equal to zero. The value of $\Delta\psi^*$ is obtained by integrating equation (2d) across the channel at a position far downstream where flow conditions are uniform

$$\Delta\psi^* = \rho_d^* q_d^* \tag{2e}$$

From Part I, ρ^* is related to the density ρ, expressed as the ratio of a characteristic density equal to the stagnation density, by

$$\rho^* = k_1\rho \tag{2f}$$

where

$$k_1 = \frac{1}{\rho_a}\sqrt{\frac{1 - \left(\frac{\rho_a q_a}{\rho_b q_b}\right)^2}{1 - \left(\frac{q_a}{q_b}\right)^2}} \tag{2g}$$

in which

$$\rho_a = \left(1 - \frac{\gamma-1}{2} q_a^{\,2}\right)^{\frac{1}{\gamma-1}} \tag{2h}$$

and

$$\rho_b = \left(1 - \frac{\gamma-1}{2} q_b^{\,2}\right)^{\frac{1}{\gamma-1}} \tag{2i}$$

where the subscripts a and b refer to quantities related to any two selected values of velocity (q_a and q_b, respectively) for which velocities the densities given by equations (2h) and (2i) are equal to the densities ρ given by equations (2f) and (2g). Also, from Part I, q^* is related to q by

$$q^* = k_2 q \tag{2j}$$

where

$$k_2 = \frac{1}{q_b}\sqrt{\frac{\left(\frac{\rho_a}{\rho_b}\right)^2 - 1}{1 - \left(\frac{\rho_a q_a}{\rho_b q_b}\right)^2}} \tag{2k}$$

For each prescribed velocity distribution along the channel walls there are an infinite number of linearized compressible flow solutions, depending on the selected values of q_a and q_b in equations (2g) and (2k). However, for values of q_a and q_b within the range of q prescribed along the channel walls (and therefore everywhere in the channel), the solutions, that is, channel shapes, probably differ only in small detail (Part I).

The values of q_a and q_b might, for example, be selected to equal the maximum and minimum values of q (which values of q must occur on the channel walls and are therefore known). Also, the values of q_a and q_b might be selected to equal the upstream and downstream velocities q_u and q_d. In this case the upstream and downstream channel widths would then satisfy continuity for a gas with the correct (arbitrary) value of γ (1.4, for example). If the upstream and downstream velocities are equal, their value and the value of some other velocity (the maximum or minimum velocity, for example) can be selected for q_a and q_b or, if desired, q_a can be equal to q_b so that

$$q_a = q_b = q$$

and

$$\rho_a = \rho_b = \rho$$

and, from Part I,

$$k_1 = \frac{1}{\rho}\sqrt{\frac{1 - \frac{\gamma+1}{2} q^2}{1 - \frac{\gamma-1}{2} q^2}} \tag{2l}$$

and

$$k_2 = \sqrt{\frac{1}{1 - \frac{\gamma+1}{2} q^2}} \tag{2m}$$

Equations (2a) and (2c) define the stream function Ψ for incompressible and linearized compressible flow, respectively. For both types of flow Ψ varies from zero along the right side of the channel, when faced in the direction of flow, to $\frac{\pi}{2}$ along the left side of the channel.

Velocity potential Φ. - If the condition of irrotational fluid motion is satisfied, a velocity potential Φ can be defined such that for incompressible flow

$$d\Phi = \frac{\pi}{2}\, d\varphi \tag{3a}$$

where, from Part I,

$$d\varphi = Q\ ds \tag{3b}$$

where s is distance in the xy-plane measured along the streamlines and expressed as the ratio of channel width downstream at infinity. For linearized compressible flow

2390

$$d\Phi = \frac{\pi}{2}\frac{d\varphi^*}{\Delta\psi^*} \tag{3c}$$

where, from Part I,

$$d\varphi^* = q^*\ ds \tag{3d}$$

Equations (3a) and (3c) define the velocity potential Φ for incompressible and linearized compressible flow, respectively.

Outline of design method. - Solutions for two-dimensional flow are boundary-value problems. That is, the solutions depend on known conditions imposed along the boundaries of the problem. In the inverse problem of channel design the geometry of the channel walls in the physical xy-plane is unknown. This unknown geometry apparently precludes the possibility of solving the problem in the physical plane and necessitates the use of some new set of coordinates, that is, a transformed plane, in which to solve the problem. These new coordinates must be such that the geometric boundaries along which the velocities are prescribed are known in the transformed plane. It is also necessary, for the method of solution employed in this report, that the coordinate system of the transformed plane be orthogonal in the physical plane. A set of coordinates that satisfies these requirements is provided by Φ and Ψ, which are orthogonal in the physical xy-plane and for which the geometric boundaries are known constant values of Ψ (equal to 0 and $\frac{\pi}{2}$) in the transformed $\Phi\Psi$-plane. The distribution of velocity as a function of Φ along these boundaries of constant Ψ is known because, if

$$Q = Q(s)$$

or

$$q = q(s)$$

is prescribed, equation (3a) or (3c) integrates to give

$$\Phi = \Phi(s)$$

from which

$$Q = Q(\Phi)$$

or

$$q = q(\Phi)$$

The technique of the proposed channel-design method is therefore to solve for the physical x,y-coordinates of the channel walls in the transformed $\Phi\Psi$-plane where the prescribed boundary conditions for the two-dimensional flow problem are known.

Channel wall coordinates. - From Part I the distribution of channel wall coordinates x and y along the boundaries of constant Ψ equal to 0 and $\frac{\pi}{2}$ in the transformed $\Phi\Psi$-plane is given by

$$x = \frac{2}{\pi} \Delta\psi^* \int \frac{\cos\,\theta}{q^*}\, d\Phi \tag{4a}$$

and

$$y = \frac{2}{\pi} \Delta\psi^* \int \frac{\sin\,\theta}{q^*}\, d\Phi \tag{4b}$$

for linearized compressible flow, and for incompressible flow

$$x = \frac{2}{\pi} \int \frac{\cos\,\theta}{Q}\, d\Phi \tag{5a}$$

and

$$y = \frac{2}{\pi} \int \frac{\sin\,\theta}{Q}\, d\Phi \tag{5b}$$

where the constants of integration are selected to give known (specified) values of x or y at one value of Φ along each boundary. Because q^* and Q are known functions of Φ from the prescribed velocity as a function of arc length along the channel walls, the shape of the channel walls in the physical xy-plane is given by equation (4) or (5) if θ is determined as a function of Φ along the channel walls (Ψ equals 0 and $\frac{\pi}{2}$). In this report the solution for θ as a function of Φ along the channel walls in the $\Phi\Psi$-plane is obtained by Green's function.

Solution by Green's Function

Continuity. - From Part I the continuity equation becomes in the transformed $\Phi\Psi$-plane

$$\frac{\partial \log_e V}{\partial \Phi} + \frac{\partial \theta}{\partial \Psi} = 0 \tag{6a}$$

where for incompressible flow

$$V = Q \tag{6b}$$

and for linearized compressible flow

$$V = \frac{q^*}{1 + \sqrt{1 + q^{*2}}} \tag{6c}$$

Irrotational motion. - From Part I the equation for irrotational motion becomes in the transformed $\Phi\Psi$-plane

$$\frac{\partial \log_e V}{\partial \Psi} - \frac{\partial \theta}{\partial \Phi} = 0 \tag{7}$$

Integral equation for $\theta(\Phi_o,\Psi_o)$. - From equations (6a) and (7)

$$\frac{\partial^2 \theta}{\partial \Phi^2} + \frac{\partial^2 \theta}{\partial \Psi^2} = 0 \tag{8}$$

so that from appendix B the value of θ at a point (Φ_o,Ψ_o) within, or on, the channel walls in the transformed $\Phi\Psi$-plane is given by the integral equation

$$\theta(\Phi_o,\Psi_o) = \frac{-1}{2\pi}\int_{-\infty}^{\infty}\left[\left(G\,\frac{\partial \log_e V}{\partial \Phi}\right)_{\frac{\pi}{2}} - \left(G\,\frac{\partial \log_e V}{\partial \Phi}\right)_0\right]d\Phi \tag{9}$$

where the subscripts 0 and $\frac{\pi}{2}$ refer to the channel wall boundaries along which Ψ is 0 and $\frac{\pi}{2}$, respectively, and G is the Green's function of the second kind for the channel, which is an infinite strip of width $\frac{\pi}{2}$ extending in the Φ-direction to $\pm\infty$.

Green's function G. - The Green's function of the second kind G for the infinite channel in the $\Phi\Psi$-plane is given along the channel wall boundaries (Ψ equals 0 and $\frac{\pi}{2}$) by (appendix C)

$$G_{0 \text{ or } \frac{\pi}{2}} = -\log_e\left[\cosh^2(\Phi-\Phi_o) - \cos^2(\Psi-\Psi_o)\right] \tag{10}$$

where (Φ,Ψ) is any point on the channel wall boundary and (Φ_o,Ψ_o) is the point in the channel or on the boundary at which θ is to be determined.

Numerical integration for $\theta(\Phi_o,\Psi_o)$. - From equations (9) and (10)

$$2\pi\,\theta(\Phi_o,\Psi_o) = \int_{-\infty}^{\infty}\left\{\frac{\partial \log_e V}{\partial\Phi}\log_e\left[\cosh^2(\Phi-\Phi_o) - \sin^2\Psi_o\right]\right\}_{\frac{\pi}{2}} d(\Phi-\Phi_o) -$$

$$\int_{-\infty}^{\infty}\left\{\frac{\partial \log_e V}{\partial\Phi}\log_e\left[\cosh^2(\Phi-\Phi_o) - \cos^2\Psi_o\right]\right\}_0 d(\Phi-\Phi_o) \tag{11}$$

in which the independent variable of integration has been changed from $d\Phi$ to $d(\Phi-\Phi_o)$ so that the origin, for purposes of integration, lies at Φ_o rather than $\Phi = 0$. If for small changes in $(\Phi-\Phi_o)$, that is for small $\Delta\Phi$, the term $\frac{\partial \log_e V}{\partial\Phi}$ may be considered constant and equal to its average value over the interval $\Delta\Phi$, then

$$\frac{\partial \log_e V}{\partial\Phi} = \frac{\Delta \log_e V}{\Delta\Phi}$$

and equation (11) becomes

$$2\pi\theta(\Phi_o,\Psi_o) = \sum_{(\Phi-\Phi_o)=-\infty}^{\infty}\left\{\frac{\Delta \log_e V}{\Delta\Phi}\int_{(\Phi-\Phi_o)}^{(\Phi-\Phi_o)+\Delta\Phi}\log_e\left[\cosh^2(\Phi-\Phi_o) - \sin^2 \Psi_o\right] d(\Phi-\Phi_o)\right\}_{\frac{\pi}{2}} -$$

$$\sum_{(\Phi-\Phi_o)=-\infty}^{\infty}\left\{\frac{\Delta \log_e V}{\Delta\Phi}\int_{(\Phi-\Phi_o)}^{(\Phi-\Phi_o)+\Delta\Phi}\log_e\left[\cosh^2(\Phi-\Phi_o) - \cos^2 \Psi_o\right] d(\Phi-\Phi_o)\right\}_0 \qquad (12)$$

2390

where the summation sign is understood to mean that the quantity within the braces is summed over the entire range of $(\Phi-\Phi_o)$ between $\pm\infty$.

Equation (12) determines θ at any point in the flow field (channel). For a point (Φ_o,Ψ_o) on the channel walls Ψ_o is equal to 0 or $\frac{\pi}{2}$ and the integrands in equation (12) become

$$2 \log_e \cosh \left|(\Phi-\Phi_o)\right|$$

or

$$2 \log_e \sinh \left|(\Phi-\Phi_o)\right|$$

so that equation (12) becomes

$$\pi\theta(\Phi_o,\Psi_o) = \sum_{(\Phi-\Phi_o)=-\infty}^{\infty}\left[\left(\frac{\Delta \log_e V}{\Delta\Phi}\Delta I\right)_{\frac{\pi}{2}} - \left(\frac{\Delta \log_e V}{\Delta\Phi}\Delta I\right)_0\right] \qquad (13a)$$

where

$$\Delta I = I_{(\Phi-\Phi_o)+\Delta\Phi} - I_{(\Phi-\Phi_o)} \qquad (13b)$$

$$\left.\begin{aligned} I_{\frac{\pi}{2}} &= \alpha \quad \text{if} \quad \Psi_o = 0 \\ I_{\frac{\pi}{2}} &= \beta \quad \text{if} \quad \Psi_o = \frac{\pi}{2} \\ I_0 &= \alpha \quad \text{if} \quad \Psi_o = \frac{\pi}{2} \\ I_0 &= \beta \quad \text{if} \quad \Psi_o = 0 \end{aligned}\right\} \tag{13c}$$

where

$$\alpha = \pm\int_0^{|(\Phi-\Phi_o)|} \log_e \cosh|(\Phi-\Phi_o)| \; d\,|(\Phi-\Phi_o)| \tag{13d}$$

$$\beta = \pm\int_0^{|(\Phi-\Phi_o)|} \log_e \sinh|(\Phi-\Phi_o)| \; d\,|(\Phi-\Phi_o)| \tag{13e}$$

where the + signs apply for positive values of $(\Phi-\Phi_o)$ and the - signs apply for negative values of $(\Phi-\Phi_o)$. Methods of evaluating α and β are given in appendix D and tabulated values are given for a wide range of $|(\Phi-\Phi_o)|$ in table I. Equation (13a) determines $\theta(\Phi_o,\Psi_o)$ at any point on the channel wall boundaries. Thus from equations (4a) and (4b) or (5a) and (5b) the coordinates for the channel wall shape in the physical xy-plane can be determined.

NUMERICAL PROCEDURE

The numerical procedure for the channel design solution by Green's function is the same, except for minor details, for incompressible and linearized compressible flow. The stepwise procedure is outlined as follows:

(1) For incompressible flow the velocity Q and for linearized compressible flow the velocity q, or which is the same thing the velocity Q and the constant downstream velocity q_d, are specified as functions of arc length along the channel walls

$$Q = Q(s) \tag{14a}$$

2390

or

$$q = q(s) \tag{14b}$$

where s is arbitrarily equal to 0 at that point along one channel wall where the velocity first begins to vary.

(2) Compute V as a function of s from equations (6b) and (14a) for incompressible flow or from equations (2j), (2k), (6c), and (14b) for linearized compressible flow.

$$V = V(s) \tag{15}$$

(3) Compute Φ as a function of s from equations (3a) and (3b) for incompressible flow or from equations (2e), (3c), (3d), and (14b) for linearized compressible flow. In equation (2e) $\rho_d{}^*$ is obtained from equations (2f) to (2i). For arbitrary distributions of Q or q equation (3a) or (3c) is integrated numerically using, for example, Simpson's one-third rule. Thus

$$\Phi = \Phi(s) \tag{16}$$

(4) From equations (15) and (16) V and Φ are known functions of s so that

$$V = V(\Phi) \tag{17}$$

Thus V is a known function of Φ along the channel wall boundaries in the transformed $\Phi\Psi$-plane.

(5) If the prescribed velocity distribution along one wall is different from that along the other, the channel will, in general, turn the flow. This turning angle $\Delta\theta$ is given by equation (E5) in appendix E. If the turning angle is unsatisfactory a new distribution of velocity as a function of s (equations (14a) and (14b)) is prescribed and steps (1) to (5) repeated until the desired value of $\Delta\theta$ is obtained. Equation (E5) is integrated numerically using Simpson's one-third rule, for example, and equation (17).

(6) The channel wall boundaries are straight parallel lines of constant Ψ equal to 0 and $\frac{\pi}{2}$, and extending to $\pm\infty$ in the Φ-direction. Along these boundaries of constant Ψ a series of equally spaced points are located at each of which the flow direction θ and the physical x,y-coordinates will be determined by numerical integration. In order to use the tables of α and β presented in this report, the point spacing $\Delta\Phi$ must be an even multiple of $\pi/24$. Thus the smallest point spacing $\pi/24$ is equal to 1/12 of the channel width $(\pi/2)$. For

a particular prescribed velocity distribution along the channel walls the accuracy of the solution increases, and so does the amount of computing, as the point spacing is reduced. The error for a given point spacing depends on the prescribed velocity distribution and its order of magnitude is given by the leading term of the error series of the formula used for numerical integration (table VIII, reference 2, for example). For the numerical example presented in this report the point spacing $\Delta\Phi$ was $\pi/12$. From equation (17)

2390

$$\frac{\Delta \log_e V}{\Delta\Phi} = \frac{(\log_e V)_{\Phi+\Delta\Phi} - (\log_e V)_{\Phi}}{\Delta\Phi} \tag{18}$$

where the subscripts Φ and $\Phi+\Delta\Phi$ refer to adjacent points along the channel boundaries.

(7) The value of θ at each point (Φ_o,Ψ_o) on the channel wall boundaries is obtained from equation (13a) in which $\frac{\Delta \log_e V}{\Delta\Phi}$ is given by equation (18) and ΔI is given by equations (13b), (13c), and table I. Note that in equation (13a) the origin has been moved to Φ_o by changing from Φ to $(\Phi-\Phi_o)$. Thus the value of $\frac{\Delta \log_e V}{\Delta\Phi}$ for a given value of $(\Phi-\Phi_o)$ varies with Φ_o.

(8) The physical x,y-coordinates at each point on the channel wall boundaries are obtained by the numerical integration of equations (5a) and (5b) for incompressible flow, or equations (4a) and (4b) for linearized compressible flow where $\Delta\psi^*$ is given by equation (2e). The constants of integration in equations (4) and (5) are selected to give known values of x and y at upstream or downstream positions where flow conditions can be considered uniform.

NUMERICAL EXAMPLE

The channel design method of this report has been applied to the design of an elbow for the same conditions as example IV of Part I. The design is for an accelerating elbow with no local decelerations of the prescribed velocities along the channel walls and with linearized compressible flow.

Prescribed velocity distribution. - The prescribed velocity distribution along the channel walls is given by q_d downstream of the elbow and by Q as a function of s along the elbow walls. The downstream velocity q_d is 0.80176. Along the inner wall (with smaller radii) of the elbow the arbitrarily prescribed velocity Q as a function of arc length s is given by

$$\left.\begin{aligned} Q &= 0.5 && (s \leq 0) \\ Q &= \frac{1}{2} + \frac{s^2}{6} - \frac{s^3}{27} && (0 \leq s \leq 3.0) \\ Q &= 1.0 && (s \geq 3.0) \end{aligned}\right\} \quad (19)$$

This velocity distribution is plotted in figure 2.

From equations (1), (2j), (3c), and (3d)

$$d\Phi = \frac{\pi}{2} \frac{k_2 q_d}{\Delta\psi^*} Q ds$$

which together with equation (19) integrates to give

$$\left.\begin{aligned} \Phi &= \frac{\pi}{2} \frac{k_2 q_d}{\Delta\psi^*} (0.5\ s) && (s \leq 0) \\ \Phi &= \frac{\pi}{2} \frac{k_2 q_d}{\Delta\psi^*} \left(\frac{s}{2} + \frac{s^3}{18} - \frac{s^4}{108}\right) && (0 \leq s \leq 3.0) \\ \Phi &= \frac{\pi}{2} \frac{k_2 q_d}{\Delta\psi^*} (-0.75+s) && (s \geq 3.0) \end{aligned}\right\} \quad (20)$$

where from equations (2h), (2i), and (2k) the constant k_2 is equal to 1.36332 and from equations (2e) to (2k) the constant $\Delta\psi^*$ is equal to 0.73782. From equations (1), (2j), (6c), (19), and (20) the variation in $\log_e V$ with Φ was obtained and is plotted in figure 3.

The distribution of velocity as a function of arc length is the same for both channel walls, but, as indicated in figure 3, the distribution on the outer wall (larger radii in xy-plane) is shifted in the positive Φ-direction an amount equal to $\frac{5}{3}\pi$ relative to the distribution on the inner wall. Thus, a velocity difference exists on the two walls at equal values of Φ in the interval $0 \leq \Phi \leq 3.333\pi$, as shown in figure 3. The greater this difference in velocity or the greater the range in Φ over which velocity differences exist, the greater is the elbow turning angle. For the prescribed velocity distribution given in figures 2 and 3 the elbow turning angle given by equation (E5) is -104.08°.

Results. - The elbow design resulting from the prescribed velocities given in figures 2 and 3 is plotted in figure 4. As indicated in table II the contour of this elbow is very nearly the same as that obtained by relaxation methods for linearized compressible flow with the same prescribed conditions (example IV, Part I).

The solution obtained by Green's function (Part II) required one experienced computer 3 days whereas the solution by relaxation methods (Part I) required about 10 days. The relaxation solutions provide additional information, such as the distribution of velocity across the channel, but for the most part this additional information is of secondary importance and the design of channels by Green's function is more rapid and therefore to be preferred over the design by relaxation methods.

SUMMARY OF RESULTS

Methods of solution by Green's function are developed for the design of two-dimensional unbranched channels with prescribed velocities as a function of arc length along the channel walls. The methods apply to incompressible and linearized-compressible, nonviscous irrotational flow. One numerical example is presented for an accelerating elbow with linearized compressible flow. The elbow shape obtained from the solution by Green's function is the same as that obtained from a solution by relaxation methods for the same prescribed conditions. The time required for the calculations was considerably less for the solution by Green's function.

Lewis Flight Propulsion Laboratory
National Advisory Committee for Aeronautics
Cleveland, Ohio, September 6, 1951

APPENDIX A

SYMBOLS

The following symbols are used in this report:

2390

$B_1, B_3, \ldots$	Bernoulli's numbers
c	constant, equation (B3)
G	Green's function of the second kind, equations (B2) and (10)
I	integral (α or β)
k_1	coefficient, equation (2g)
k_2	coefficient, equation (2k)
l	length of closed boundary
n	distance in xy-plane measured normal to direction of flow (expressed as ratio of characteristic length equal to channel width downstream at infinity)
Q	velocity (expressed as ratio of characteristic velocity equal to constant channel velocity downstream at infinity)
q	velocity (expressed as ratio of stagnation speed of sound)
q^*	velocity used in linearized compressible flow and related to q by equation (2j)
r	distance from any point in $\Phi\Psi$-plane to point (Φ_o, Ψ_o) at which logarithmic singularity exists
s	distance in xy-plane measured along direction of flow (expressed as ratio of characteristic length equal to channel width downstream at infinity)
V	velocity parameter defined by equations (6b) and (6c) for incompressible and linearized compressible flow, respectively

w, w_1, w_2	complex functions defined by equations (C3), (C1a), and (C2a), respectively
x, y	Cartesian coordinates in physical plane (expressed as ratios of characteristic length equal to channel width downstream at infinity)
z	complex coordinate, equation (C1b)
$\bar{z}$	conjugate of z
α	integral, equation (13d)
β	integral, equation (13e)
γ	ratio of specific heats
Δ	finite increment
θ	flow direction in physical xy-plane (measured in counterclockwise direction from positive x-axis)
$\Delta\theta$	channel turning angle, equation (E1)
ρ	density (expressed as ratio of stagnation density)
ρ^*	density used in linearized compressible flow and related to ρ by equation (2f)
Φ	velocity potential used as Cartesian coordinate in transformed $\Phi\Psi$-plane and related to φ or φ^* by equation (3a) or (3c), respectively
φ and φ^*	velocity potential for incompressible and linearized compressible flow, respectively, equations (3b) and (3d)
Ψ	stream function used as Cartesian coordinate in transformed $\Phi\Psi$-plane and related to ψ or ψ^* by equation (2a) or (2c), respectively
ψ and ψ^*	stream function for incompressible and linearized compressible flow, respectively, equations (2b) and (2d)
$\Delta\psi^*$	boundary value of ψ^*, for linearized compressible flow, along left channel wall when faced in the direction of flow, equation (2e)

ω	any harmonic function in $\Phi\Psi$-plane

Subscripts:

a,b	quantities related to any two selected values of velocity (q_a and q_b, respectively) for which densities given by equations (2h) and (2i) are equal to densities given by equations (2f) and (2g)
d	conditions downstream at infinity
o	point in $\Phi\Psi$-plane at which θ is determined
u	conditions upstream at infinity
$(\Phi-\Phi_o)$	point at $(\Phi-\Phi_o)$ on either channel wall boundary
$(\Phi-\Phi_o)+\Delta\Phi$	point at $\left[(\Phi-\Phi_o)+\Delta\Phi\right]$ on either channel wall boundary
0	boundary along which Ψ equals 0
$\frac{\pi}{2}$	boundary along which Ψ equals $\frac{\pi}{2}$

2390

APPENDIX B

INTEGRAL EQUATION FOR $\theta(\Phi_o,\Psi_o)$

If the distribution of the angle $\theta(\Phi,\Psi)$ in the transformed $\Phi\Psi$-plane is harmonic, that is, satisfies equation (8) within and on the channel walls (Ψ equals 0 and $\frac{\pi}{2}$), then from Green's theorem and the theorem of mean value it can be shown that the value of θ at a point (Φ_o,Ψ_o) within (or on) the channel walls is given by (reference 3, p. 204, for example)

$$\theta(\Phi_o,\Psi_o) = \frac{1}{2\pi}\left[\int_{-\infty}^{\infty}\left(\theta\,\frac{\partial G}{\partial \Psi} - G\,\frac{\partial \theta}{\partial \Psi}\right)_0 d\Phi - \int_{\infty}^{-\infty}\left(-\,\theta\,\frac{\partial G}{\partial \Psi} + G\,\frac{\partial \theta}{\partial \Psi}\right)_{\frac{\pi}{2}} d\Phi\right] \tag{B1}$$

where the two integrals on the right side of equation (B1) represent the line integral around the channel walls in the counterclockwise direction with the signs adjusted so that $\frac{\partial}{\partial \Psi}$ represents the inner normal to the path of integration.

The function $G(\Phi,\Psi)$ in equation (B1) is of the form (reference 3, p. 204).

$$G(\Phi,\Psi) = \log_e \frac{1}{r} + \omega(\Phi,\Psi) \tag{B2}$$

where r is the distance from any point (Φ,Ψ) to the point (Φ_o,Ψ_o) and where $\omega(\Phi,\Psi)$ is an arbitrary function that is harmonic within and on the channel walls. (Thus from equation (B2), $G(\Phi,\Psi)$ is harmonic within and on the channel walls except at the point (Φ_o,Ψ_o) where a logarithmic singularity exists.) Because the harmonic function $\omega(\Phi,\Psi)$ is arbitrary, the function $G(\Phi,\Psi)$ can be selected so that along the channel wall boundaries (Ψ equals 0 and $\frac{\pi}{2}$) $\frac{\partial G}{\partial \Psi}$ is a constant c given by the following equation (obtained from notes presented by Tamarkin and Feller in the 1941 Summer Session for Advanced Instruction and Research in Mechanics at Brown Univ.):

$$c = \frac{2\pi}{l} \tag{B3}$$

where l is the length of the path along which the line integral is taken. For the path under consideration l is infinite and therefore

$G(\Phi,\Psi)$ can be selected so that $\frac{\partial G}{\partial \Psi}$ is zero along the channel walls. A function with this property is called a Green's function of the second kind. Equation (B1) becomes

$$\theta(\Phi_o,\Psi_o) = \frac{1}{2\pi}\int_{-\infty}^{\infty}\left[\left(G\frac{\partial\theta}{\partial\Psi}\right)_{\frac{\pi}{2}} - \left(G\frac{\partial\theta}{\partial\Psi}\right)_{0}\right]d\Phi$$

or, combined with equation (6a)

$$\theta(\Phi_o,\Psi_o) = \frac{-1}{2\pi}\int_{-\infty}^{\infty}\left[\left(G\frac{\partial \log_e V}{\partial\Phi}\right)_{\frac{\pi}{2}} - \left(G\frac{\partial \log_e V}{\partial\Phi}\right)_{0}\right]d\Phi \qquad (9)$$

Along the channel walls $\frac{\partial \log_e V}{\partial \Phi}$ is known from the prescribed velocity distribution so that, after the proper Green's function G has been determined (appendix C), equation (9) determines the value of θ at any point (Φ_o,Ψ_o). The value of $\theta(\Phi_o,\Psi_o)$ given by equation (9) can be adjusted by an arbitrary constant of integration to give a specified value of θ at one point in the flow field.

APPENDIX C

GREEN'S FUNCTION OF SECOND KIND

From appendix B Green's function of the second kind G satisfies the condition

$$\frac{\partial G}{\partial \Psi} = 0$$

along the channel walls, which are straight and parallel boundaries (Ψ equals 0 and $\frac{\pi}{2}$) extending to $\pm\infty$ in the Φ-direction, and satisfies the equation

$$\frac{\partial^2 G}{\partial \Phi^2} + \frac{\partial^2 G}{\partial \Psi^2} = 0$$

everywhere in the channel except at the point (Φ_o,Ψ_o) where G has a logarithmic pole. For these conditions the Green's function G can be obtained by analogy from the velocity potential for incompressible flow into a point sink at (Φ_o,Ψ_o) between straight parallel boundaries at Ψ equal to 0 and $\frac{\pi}{2}$. The logarithmic pole for G at (Φ_o,Ψ_o) corresponds to the point sink and the condition $\frac{\partial G}{\partial \Psi} = 0$ at the boundaries corresponds to zero velocity, that is, no flow normal to the boundaries.

The velocity potential for fluid flow with the boundary conditions just described is obtained from two infinite series of point sinks with the sinks of each series spaced π distance apart in the Ψ-direction and the two series arranged by the method of images in such a manner that no flow crosses the boundaries, that is $\frac{\partial G}{\partial \Psi} = 0$. This arrangement of point sinks is shown in figure 5.

The complex function w_1 for the first infinite series of point sinks is given by (reference 4, p. 112, for example)

$$w_1 = -\log_e \sinh (z-z_o) \tag{C1a}$$

where

$$z = \Phi + i\Psi \tag{C1b}$$

The complex function w_2 for the second infinite series of point sinks (mirror image of the first series in order to prevent flow across the boundaries Ψ equals 0 and $\frac{\pi}{2}$) is given by

$$w_2 = -\log_e \sinh (z-\overline{z}_o) \tag{C2a}$$

2390

where

$$\overline{z} = \Phi - i\Psi \tag{C2b}$$

The complex function w for the combined flow becomes from equations (C1a) to (C2b)

$$w = w_1 + w_2 = -\log_e \sinh \left[(\Phi-\Phi_o) + i (\Psi-\Psi_o)\right] - \log_e \sinh \left[(\Phi-\Phi_o) + i (\Psi+\Psi_o)\right] \tag{C3}$$

The Green's function of the second kind G corresponds to the velocity potential for the incompressible flow and is therefore given by the real part of equation (C3)

$$G = -\frac{1}{2} \log_e \left[\cosh^2 (\Phi-\Phi_o) - \cos^2 (\Psi-\Psi_o)\right] \left[\cosh^2 (\Phi-\Phi_o) - \cos^2 (\Psi+\Psi_o)\right] \tag{C4}$$

But along the channel walls Ψ is equal to 0 or $\frac{\pi}{2}$ so that

$$\cos^2 (\Psi+\Psi_o) = \cos^2 (\Psi-\Psi_o)$$

and equation (C4) becomes

$$G_{0 \text{ or } \frac{\pi}{2}} = -\log_e \left[\cosh^2 (\Phi-\Phi_o) - \cos^2 (\Psi-\Psi_o)\right] \tag{10}$$

Equation (10) gives the Green's function of the second kind along the channel walls (straight parallel lines of constant Ψ equal to 0 and $\frac{\pi}{2}$ and extending to $\pm\infty$ in the Φ-direction).

APPENDIX D

EVALUATION OF α AND β

Several techniques, depending on the magnitude of the upper limit $|(\Phi-\Phi_o)|$, were used to evaluate the integrals α and β given by equations (13d) and (13e). Each integral is treated separately in this appendix and the values of $(\Phi-\Phi_o)$ for the upper limit $|(\Phi-\Phi_o)|$ are considered positive. For negative values of $(\Phi-\Phi_o)$ the magnitudes of I (that is, of α or β) are equal for corresponding values of $|(\Phi-\Phi_o)|$ but opposite in sign. As a result the values of ΔI have the same sign.

Integral α

<u>Small and medium values of $(\Phi-\Phi_o)$.</u> - For small and medium values of the upper limit of integration $(\Phi-\Phi_o)$ in equation (13d), that is, for $0 \leq (\Phi-\Phi_o) \leq 60\ \pi/24$, the integral α is evaluated by Simpson's one-third rule using increments of $(\Phi-\Phi_o)$ equal to $\pi/48$.

<u>Large values of $(\Phi-\Phi_o)$.</u> - For large values of $(\Phi-\Phi_o)$ that is for $(\Phi-\Phi_o) > 60\ \pi/24$, the integrand in equation (13d) becomes

$$\log_e \cosh\ (\Phi-\Phi_o) \approx (\Phi-\Phi_o) - \log_e 2 \tag{D1}$$

so that equation (13d) becomes

$$\begin{aligned}\alpha &\approx \int_0^{60\pi/24} \log_e \cosh\ (\Phi-\Phi_o)\ d(\Phi-\Phi_o) + \\ &\quad \int_{60\pi/24}^{(\Phi-\Phi_o)} \left[(\Phi-\Phi_o) - \log_e 2\right] d(\Phi-\Phi_o) \\ &\approx 25.809782 + \left[\frac{(\Phi-\Phi_o)^2}{2} - 0.693147\ (\Phi-\Phi_o) - 25.398552\right] \\ &\approx 0.411230 - 0.693147\ (\Phi-\Phi_o) + \frac{1}{2}\ (\Phi-\Phi_o)^2 \end{aligned} \tag{D2}$$

Equation (D2) gives values of α for values of $(\Phi-\Phi_o)$ equal to or greater than $60\pi/24$. Values of the integral α are tabulated in table I for a range of $|(\Phi-\Phi_o)|$ between 0 and $100\pi/24$ in increments of $\pi/24$. For negative values of $(\Phi-\Phi_o)$ the sign of α is negative.

2390

Integral β

Small values of $(\Phi-\Phi_o)$. - For $(\Phi-\Phi_o)$ equal to zero the integrand of equation (13e) becomes minus infinity so that Simpson's one-third rule cannot be used to evaluate β in this region of $(\Phi-\Phi_o)$, as was done for α. However, equation (13e) integrates by parts to give

$$\int_0^{(\Phi-\Phi_o)} \log_e \sinh (\Phi-\Phi_o)\, d(\Phi-\Phi_o)$$

$$= (\Phi-\Phi_o) \log_e \sinh (\Phi-\Phi_o) -$$

$$\int_0^{(\Phi-\Phi_o)} (\Phi-\Phi_o) \operatorname{ctnh} (\Phi-\Phi_o)\, d(\Phi-\Phi_o) \tag{D3}$$

where the integrand $(\Phi-\Phi_o) \operatorname{ctnh} (\Phi-\Phi_o)$ on the right side of equation (D3) can be expanded in the following series form:

$$(\Phi-\Phi_o) \operatorname{ctnh} (\Phi-\Phi_o) = 1 + \frac{2^2B_1 (\Phi-\Phi_o)^2}{2!} - \frac{2^4B_3 (\Phi-\Phi_o)^4}{4!} + \frac{2^6B_5 (\Phi-\Phi_o)^6}{6!} -$$

$$\frac{2^8B_7 (\Phi-\Phi_o)^8}{8!} + \frac{2^{10}B_9 (\Phi-\Phi_o)^{10}}{10!} - \frac{2^{12}B_{11} (\Phi-\Phi_o)^{12}}{12!} + \ldots \tag{D4}$$

where B_1, B_3, and so forth, are called Bernoulli's numbers (reference 5, p. 90, for example). From equations (D3) and (D4)

$$\beta = (\Phi-\Phi_o) \log_e \sinh (\Phi-\Phi_o) - (\Phi-\Phi_o) - \frac{(\Phi-\Phi_o)^3}{9} + \frac{(\Phi-\Phi_o)^5}{225} - \frac{2(\Phi-\Phi_o)^7}{6615} +$$

$$\frac{(\Phi-\Phi_o)^9}{42,525} - \frac{2(\Phi-\Phi_o)^{11}}{1,029,105} + \frac{1382\ (\Phi-\Phi_o)^{13}}{8,300,667,375} - \ldots \tag{D5}$$

2390

Equation (D5) was used to obtain β as a function of $(\Phi-\Phi_o)$ for $0 \leq (\Phi-\Phi_o) \leq 8\pi/24$.

Medium values of $(\Phi-\Phi_o)$. - For medium values of the upper limit of integration $(\Phi-\Phi_o)$ in equation (13e), that is, for $8\pi/24 < (\Phi-\Phi_o) \leq 60\pi/24$, the integral β is evaluated by Simpson's one-third rule as was done for α.

Large values of $(\Phi-\Phi_o)$. - For large values of $(\Phi-\Phi_o)$, that is, for $(\Phi-\Phi_o) > 60\pi/24$, the integrand in equation (13e) becomes

$$\log_e \sinh (\Phi-\Phi_o) \approx (\Phi-\Phi_o) - \log_e 2 \tag{D6}$$

so that equation (13e) becomes

$$\beta \approx \int_0^{60\pi/24} \log_e \sinh (\Phi-\Phi_o)\, d(\Phi-\Phi_o) +$$

$$\int_{60\pi/24}^{(\Phi-\Phi_o)} \left[(\Phi-\Phi_o) - \log_e 2\right] d(\Phi-\Phi_o)$$

$$\approx 24.576082 + \left[\frac{(\Phi-\Phi_o)^2}{2} - 0.693147\ (\Phi-\Phi_o) - 25.398552\right]$$

$$\approx -0.822470 - 0.693147\ (\Phi-\Phi_o) + \frac{1}{2}(\Phi-\Phi_o)^2 \tag{D7}$$

Equation (D7) gives values of β for values of $(\Phi-\Phi_o)$ equal to or greater than $60\pi/24$. Values of the integral β are tabulated in table I for a range of $|(\Phi-\Phi_o)|$ between 0 and $100\pi/24$ in increments of $\pi/24$. For negative values of $(\Phi-\Phi_o)$ the sign of β changes.

APPENDIX E

CHANNEL TURNING ANGLE

If the prescribed velocity distribution along one channel wall differs from the distribution along the other wall, then in general the channel deflects an amount $\Delta\theta$, which is the difference in flow direction far downstream and far upstream of the region in which the prescribed velocity distribution varies. Thus,

$$\Delta\theta = \theta_d - \theta_u \tag{E1}$$

For large values of $|(\Phi-\Phi_o)|$ such as occur far upstream and far downstream of the region in which the prescribed velocity varies along the channel walls

$$\cosh^2 (\Phi-\Phi_o) \gg \cos^2 (\Psi-\Psi_o)$$

so that from equation (10)

$$G_0 = G_{\frac{\pi}{2}} = 2 \left[|(\Phi-\Phi_o)| - \log_e 2\right] \tag{E2}$$

Far upstream $\Phi_o<\Phi$ so that

$$|(\Phi-\Phi_o)| = (\Phi-\Phi_o)$$

and because V is harmonic

$$\int_{-\infty}^{\infty}\left[\left(\frac{\partial \log_e V}{\partial\Phi}\right)_{\frac{\pi}{2}} - \left(\frac{\partial \log_e V}{\partial\Phi}\right)_0\right] d\Phi = 0$$

so that equation (E2) substituted in equation (9) gives

$$\theta_u = \frac{1}{\pi} \int_{-\infty}^{\infty} \Phi \left[\left(\frac{\partial \log_e V}{\partial\Phi}\right)_{\frac{\pi}{2}} - \left(\frac{\partial \log_e V}{\partial\Phi}\right)_0\right] d\Phi \tag{E3}$$

Likewise, far downstream $\Phi_o > \Phi$ so that

$$|(\Phi-\Phi_o)| = -(\Phi-\Phi_o)$$

2390

and equation (E2) substituted in equation (9) gives

$$\theta_d = \frac{-1}{\pi}\int_{-\infty}^{\infty}\Phi\left[\left(\frac{\partial \log_e V}{\partial\Phi}\right)_{\frac{\pi}{2}} - \left(\frac{\partial \log_e V}{\partial\Phi}\right)_0\right]d\Phi \qquad \text{(E4)}$$

From equations (E1), (E3), and (E4)

$$\Delta\theta = \frac{-2}{\pi}\int_{-\infty}^{\infty}\Phi\left[\left(\frac{\partial \log_e V}{\partial\Phi}\right)_{\frac{\pi}{2}} - \left(\frac{\partial \log_e V}{\partial\Phi}\right)_0\right]d\Phi \qquad \text{(E5)}$$

Equation (E5) determines the channel turning angle $\Delta\theta$.

REFERENCES

1. Stanitz, John D.: Design of Two-Dimensional Channels with Prescribed Velocity Distributions Along the Channel Walls. I - Relaxation Solutions. NACA TN 2593, 1952.

2. Southwell, R. V.: Relaxation Methods in Theoretical Physics. Clarendon Press (Oxford), 1946.

3. Osgood, William Fogg: Functions of a Complex Variable. G. E. Stechert & Co. (New York), 1942.

4. Streeter, Victor L.: Fluid Dynamics. McGraw-Hill Book Co., Inc. (New York), 1948.

5. Peirce, B. O.: A Short Table of Integrals. Ginn and Company (Boston), 1929.

TABLE I - TABULATED VALUES OF THE INTEGRALS α AND β FOR A RANGE OF $|(\Phi-\Phi_o)|$

[Computational methods given in appendix D.]

$\|(\Phi-\Phi_o)\|$	α (1)	$\Delta I = \Delta\alpha$		β (1)	$\Delta I = \Delta\beta$	
		$\Delta_1\alpha$ ($\Delta\Phi=\pi/24$)	$\Delta_2\alpha$ ($\Delta\Phi=2\pi/24$)		$\Delta_1\beta$ ($\Delta\Phi=\pi/24$)	$\Delta_2\beta$ ($\Delta\Phi=2\pi/24$)
0	0			0		
1(π/24)	0.000373	0.000373	0.002970	-0.396937	-0.396937	-0.611660
2(π/24)	.002970	.002597		-.611660	-.214723	
3(π/24)	.009942	.006972	.020331	-.756406	-.144746	-.242791
4(π/24)	.023301	.013359		-.854451	-.098045	
5(π/24)	.044875	.021574	.052976	-.916486	-.062035	-.094079
6(π/24)	.076277	.031402		-.948530	-.032044	
7(π/24)	.118897	.042620	.097632	-.954346	-.005816	.012092
8(π/24)	.173909	.055012		-.936438	.017908	
9(π/24)	.242283	.068374	.150903	-.896542	.039896	.100542
10(π/24)	.324812	.082529		-.835896	.060646	
11(π/24)	.422136	.097324	.209951	-.755399	.080497	.180181
12(π/24)	.534763	.112627		-.655715	.099684	
13(π/24)	.663098	.128335	.272697	-.537338	.118377	.255075
14(π/24)	.807460	.144362		-.400640	.136698	
15(π/24)	.968096	.160636	.337741	-.245901	.154739	.327305
16(π/24)	1.145201	.177105		-.073335	.172566	
17(π/24)	1.338926	.193725	.404188	.116897	.190232	.398006
18(π/24)	1.549389	.210463		.324671	.207774	
19(π/24)	1.776679	.227290	.471478	.549892	.225221	.467817
20(π/24)	2.020867	.244188		.792488	.242596	
21(π/24)	2.282008	.261141	.539276	1.052403	.259915	.537106
22(π/24)	2.560143	.278135		1.329594	.277191	
23(π/24)	2.855304	.295161	.607373	1.624029	.294435	.606089
24(π/24)	3.167516	.312212		1.935683	.311654	
25(π/24)	3.496799	.329283	.675652	2.264536	.328853	.674890
26(π/24)	3.843168	.346369		2.610573	.346037	
27(π/24)	4.206633	.363465	.744035	2.973783	.363210	.743585
28(π/24)	4.587203	.380570		3.354158	.380375	
29(π/24)	4.984885	.397682	.812482	3.751689	.397531	.812215
30(π/24)	5.399685	.414800		4.166373	.414684	
31(π/24)	5.831607	.431922	.880967	4.598205	.431832	.880808
32(π/24)	6.280652	.449045		5.047181	.448976	
33(π/24)	6.746825	.466173	.949474	5.513301	.466120	.949380
34(π/24)	7.230126	.483301		5.996561	.483260	
35(π/24)	7.730557	.500431	1.017993	6.496961	.500400	1.017938
36(π/24)	8.248119	.517562		7.014499	.517538	
37(π/24)	8.782813	.534694	1.086521	7.549175	.534676	1.086488
38(π/24)	9.334640	.551827		8.100987	.551812	
39(π/24)	9.903600	.568960	1.155053	8.669936	.568949	1.155034
40(π/24)	10.489693	.586093		9.256021	.586085	
41(π/24)	11.092920	.603227	1.223588	9.859241	.603220	1.223576
42(π/24)	11.713281	.620361		10.479597	.620356	
43(π/24)	12.350777	.637496	1.292125	11.117089	.637492	1.292118
44(π/24)	13.005406	.654629		11.771715	.654626	
45(π/24)	13.677170	.671764	1.360662	12.443477	.671762	1.360658
46(π/24)	14.366068	.688898		13.132373	.688896	
47(π/24)	15.072101	.706033	1.429200	13.838405	.706032	1.429198
48(π/24)	15.795268	.723167		14.561571	.723166	
49(π/24)	16.535571	.740303	1.497739	15.301873	.740302	1.497738
		.757436			.757436	

(1) For negative values of $(\Phi-\Phi_o)$ the signs of α and β change, but the signs of $\Delta\alpha$ and $\Delta\beta$ remain unchanged.

2390

2390

TABLE I - TABULATED VALUES OF THE INTEGRALS α AND β FOR A RANGE OF $|(\Phi-\Phi_o)|$ - Concluded

[Computational methods given in appendix D.]

$\|(\Phi-\Phi_o)\|$	α (1)	$\Delta I = \Delta\alpha$		β (1)	$\Delta I = \Delta\beta$	
		$\Delta_1\alpha$ ($\Delta\Phi=\pi/24$)	$\Delta_2\alpha$ ($\Delta\Phi=2\pi/24$)		$\Delta_1\beta$ ($\Delta\Phi=\pi/24$)	$\Delta_2\beta$ ($\Delta\Phi=2\pi/24$)
$50(\pi/24)$	17.293007			16.059309		
$51(\pi/24)$	18.067579	.774572	1.566278	16.833880	.774571	1.566276
$52(\pi/24)$	18.859285	.791706		17.625585	.791705	
$53(\pi/24)$	19.668125	.808840	1.634816	18.434426	.808841	1.634816
$54(\pi/24)$	20.494101	.825976		19.260401	.825975	
$55(\pi/24)$	21.337211	.843110	1.703355	20.103511	.843110	1.703354
$56(\pi/24)$	22.197456	.860245		20.963755	.860244	
$57(\pi/24)$	23.074835	.877379	1.771893	21.841135	.877380	1.771894
$58(\pi/24)$	23.969349	.894514		22.735649	.894514	
$59(\pi/24)$	24.880998	.911649	1.840433	23.647298	.911649	1.840433
$60(\pi/24)$	25.809782	.928784		24.576082	.928784	
$61(\pi/24)$	26.755694	.945912	1.908968	25.521994	.945912	1.908968
$62(\pi/24)$	27.718750	.963056		26.485050	.963056	
$63(\pi/24)$	28.698940	.980190	1.977507	27.465240	.980190	1.977507
$64(\pi/24)$	29.696257	.997317		28.462557	.997317	
$65(\pi/24)$	30.710717	1.014460	2.046044	29.477017	1.014460	2.046044
$66(\pi/24)$	31.742311	1.031594		30.508611	1.031594	
$67(\pi/24)$	32.791033	1.048722	2.114585	31.557333	1.048722	2.114585
$68(\pi/24)$	33.856896	1.065863		32.623196	1.065863	
$69(\pi/24)$	34.939895	1.082999	2.183123	33.706195	1.082999	2.183123
$70(\pi/24)$	36.040029	1.100134		34.806329	1.100134	
$71(\pi/24)$	37.157289	1.117260	2.251663	35.923589	1.117260	2.251663
$72(\pi/24)$	38.291692	1.134403		37.057992	1.134403	
$73(\pi/24)$	39.443230	1.151538	2.320201	38.209530	1.151538	2.320201
$74(\pi/24)$	40.611893	1.168663		39.378193	1.168663	
$75(\pi/24)$	41.797701	1.185808	2.388740	40.564001	1.185808	2.388740
$76(\pi/24)$	43.000643	1.202942		41.766943	1.202942	
$77(\pi/24)$	44.220710	1.220067	2.457279	42.987010	1.220067	2.457279
$78(\pi/24)$	45.457922	1.237212		44.224222	1.237212	
$79(\pi/24)$	46.712269	1.254347	2.525818	45.478569	1.254347	2.525818
$80(\pi/24)$	47.983750	1.271481		46.750050	1.271481	
$81(\pi/24)$	49.272356	1.288606	2.594357	48.038656	1.288606	2.594357
$82(\pi/24)$	50.578107	1.305751		49.344407	1.305751	
$83(\pi/24)$	51.900992	1.322885	2.662895	50.667292	1.322885	2.662895
$84(\pi/24)$	53.241002	1.340010		52.007302	1.340010	
$85(\pi/24)$	54.598158	1.357156	2.731435	53.364458	1.357156	2.731435
$86(\pi/24)$	55.972447	1.374289		54.738747	1.374289	
$87(\pi/24)$	57.363861	1.391414	2.799974	56.130161	1.391414	2.799973
$88(\pi/24)$	58.772421	1.408560		57.538720	1.408560	
$89(\pi/24)$	60.198115	1.425694	2.868512	58.964415	1.425694	2.868513
$90(\pi/24)$	61.640933	1.442818		60.407233	1.442818	
$91(\pi/24)$	63.100897	1.459964	2.937052	61.867197	1.459964	2.937052
$92(\pi/24)$	64.577995	1.477098		63.344295	1.477098	
$93(\pi/24)$	66.072228	1.494233	3.005590	64.838528	1.494233	3.005590
$94(\pi/24)$	67.583585	1.511357		66.349885	1.511357	
$95(\pi/24)$	69.112088	1.528503	3.074130	67.878388	1.528503	3.074130
$96(\pi/24)$	70.657725	1.545637		69.424025	1.545637	
$97(\pi/24)$	72.220486	1.562761	3.142668	70.986786	1.562761	3.142668
$98(\pi/24)$	73.800393	1.579907		72.566693	1.579907	
$99(\pi/24)$	75.397435	1.597042	3.211206	74.163735	1.597042	3.211206
$100(\pi/24)$ (2)	77.011599	1.614164		75.777899	1.614164	

(1) For negative values of $(\Phi-\Phi_o)$ the signs of α and β change, but the signs of $\Delta\alpha$ and $\Delta\beta$ remain unchanged.

(2) For values of $|(\Phi-\Phi_o)| > 100(\pi/24)$ use equation (D2) for α and equation (D7) for β.

2390

TABLE II - COMPARISON OF ELBOW DESIGNS OBTAINED FROM SOLUTIONS BY RELAXATION METHODS AND BY GREEN'S FUNCTION

[Linearized compressible flow; prescribed velocity distribution given in figs. 2 and 3.]

Φ	Ψ = 0 (Inner wall)								Ψ = π/2 (Outer wall)							
	Q	q	Solution by relaxation methods (Part I)			Solution by Green's function (Part II)			Q	q	Solution by relaxation methods (Part I)			Solution by Green's function (Part II)		
			x	y	θ (deg)	x	y	θ (deg)			x	y	θ (deg)	x	y	θ (deg)
-22(π/24)	0.5000	0.4009	-2.466	-0.769	0	-2.466	-0.769	0	0.5000	0.4009	-2.466	.770	0	-2.466	.770	0
-20(π/24)	.5000	.4009	-2.241	-.769	.01	-2.241	-.769	.01	.5000	.4009	-2.241	.770	-.01	-2.241	.770	-.01
-18(π/24)	.5000	.4009	-2.016	-.769	.01	-2.016	-.769	.01	.5000	.4009	-2.016	.770	-.01	-2.016	.770	-.01
-16(π/24)	.5000	.4009	-1.791	-.769	.02	-1.791	-.769	.02	.5000	.4009	-1.791	.770	-.02	-1.791	.770	-.02
-14(π/24)	.5000	.4009	-1.566	-.768	.03	-1.566	-.768	.03	.5000	.4009	-1.566	.770	-.03	-1.566	.770	-.03
-12(π/24)	.5000	.4009	-1.341	-.768	.05	-1.341	-.768	.05	.5000	.4009	-1.341	.769	-.05	-1.341	.770	-.05
-10(π/24)	.5000	.4009	-1.116	-.768	.08	-1.116	-.768	.08	.5000	.4009	-1.116	.769	-.08	-1.116	.769	-.08
-8(π/24)	.5000	.4009	-.891	-.768	.14	-.891	-.768	.14	.5000	.4009	-.891	.769	-.13	-.891	.769	-.13
-6(π/24)	.5000	.4009	-.666	-.767	.24	-.666	-.767	.24	.5000	.4009	-.666	.768	-.21	-.666	.768	-.22
-4(π/24)	.5000	.4009	-.441	-.766	.40	-.441	-.766	.41	.5000	.4009	-.441	.767	-.35	-.441	.767	-.36
-2(π/24)	.5000	.4009	-.216	-.763	.70	-.216	-.763	.74	.5000	.4009	-.216	.765	-.56	-.216	.765	-.59
0	.5000	.4009	.008	-.760	1.31	.010	-.759	1.52	.5000	.4009	.009	.763	-.92	.009	.762	-.94
2(π/24)	.5079	.4072	.233	-.752	2.82	.233	-.751	2.76	.5000	.4009	.234	.758	-1.45	.234	.758	-1.48
4(π/24)	.5293	.4243	.450	-.739	3.88	.449	-.738	3.76	.5000	.4009	.459	.751	-2.22	.459	.750	-2.24
6(π/24)	.5599	.4489	.656	-.724	4.00	.656	-.724	3.89	.5000	.4009	.684	.740	-3.28	.684	.740	-3.29
8(π/24)	.5962	.4780	.851	-.712	3.17	.850	-.713	3.07	.5000	.4009	.908	.725	-4.65	.908	.724	-4.68
10(π/24)	.6354	.5094	1.033	-.704	1.44	1.033	-.705	1.38	.5000	.4009	1.132	.703	-6.41	1.132	.702	-6.43
12(π/24)	.6754	.5415	1.205	-.703	-.98	1.205	-.704	-1.04	.5000	.4009	1.355	.674	-8.52	1.355	.673	-8.56
14(π/24)	.7149	.5732	1.366	-.710	-4.00	1.367	-.711	-4.04	.5000	.4009	1.577	.636	-11.04	1.577	.635	-11.06
16(π/24)	.7531	.6038	1.519	-.725	-7.48	1.519	-.727	-7.51	.5000	.4009	1.797	.587	-13.91	1.797	.586	-13.94
18(π/24)	.7894	.6329	1.663	-.749	-11.35	1.663	-.750	-11.37	.5000	.4009	2.013	.527	-17.13	2.013	.526	-17.16
20(π/24)	.8235	.6602	1.798	-.781	-15.52	1.799	-.783	-15.54	.5000	.4009	2.226	.455	-20.67	2.226	.453	-20.69
22(π/24)	.8550	.6855	1.926	-.822	-19.96	1.926	-.823	-19.98	.5000	.4009	2.434	.368	-24.49	2.434	.367	-24.52
24(π/24)	.8838	.7086	2.046	-.871	-24.62	2.046	-.871	-24.63	.5000	.4009	2.635	.268	-28.58	2.635	.266	-28.59
26(π/24)	.9097	.7293	2.157	-.928	-29.46	2.158	-.929	-29.47	.5000	.4009	2.829	.153	-32.89	2.828	.152	-32.90
28(π/24)	.9326	.7477	2.261	-.993	-34.45	2.261	-.994	-34.46	.5000	.4009	3.013	.024	-37.40	3.012	.022	-37.41
30(π/24)	.9524	.7636	2.356	-1.064	-39.56	2.356	-1.066	-39.57	.5000	.4009	3.186	-.120	-42.08	3.185	-.122	-42.09
32(π/24)	.9690	.7769	2.443	-1.143	-44.76	2.443	-1.144	-44.77	.5000	.4009	3.346	-.278	-46.93	3.346	-.279	-46.94
34(π/24)	.9822	.7875	2.521	-1.228	-50.02	2.521	-1.229	-50.01	.5000	.4009	3.492	-.449	-51.93	3.492	-.450	-51.94
36(π/24)	.9919	.7953	2.590	-1.318	-55.27	2.590	-1.320	-55.27	.5000	.4009	3.623	-.632	-57.08	3.623	-.633	-57.10
38(π/24)	.9979	.8001	2.650	-1.414	-60.49	2.650	-1.415	-60.47	.5000	.4009	3.736	-.826	-62.44	3.736	-.828	-62.49
40(π/24)	1.0000	.8018	2.701	-1.514	-65.55	2.701	-1.516	-65.51	.5000	.4009	3.830	-1.030	-68.16	3.829	-1.034	-68.37
42(π/24)	1.0000	.8018	2.743	-1.619	-70.32	2.744	-1.620	-70.29	.5079	.4072	3.901	-1.242	-74.80	3.901	-1.244	-74.75
44(π/24)	1.0000	.8018	2.777	-1.726	-74.81	2.777	-1.727	-74.78	.5293	.4243	3.947	-1.455	-81.03	3.945	-1.456	-80.91
46(π/24)	1.0000	.8018	2.803	-1.836	-78.97	2.803	-1.837	-78.96	.5599	.4489	3.969	-1.661	-86.33	3.969	-1.662	-86.23
48(π/24)	1.0000	.8018	2.820	-1.947	-82.82	2.821	-1.948	-82.80	.5962	.4780	3.974	-1.856	-90.69	3.975	-1.856	-90.59
50(π/24)	1.0000	.8018	2.831	-2.059	-86.28	2.831	-2.059	-86.26	.6354	.5094	3.966	-2.038	-94.16	3.967	-2.040	-94.09
52(π/24)	1.0000	.8018	2.835	-2.171	-89.37	2.836	-2.172	-89.34	.6754	.5415	3.950	-2.209	-96.93	3.951	-2.210	-96.88
54(π/24)	1.0000	.8018	2.834	-2.283	-92.07	2.834	-2.285	-92.04	.7149	.5732	3.927	-2.369	-99.11	3.928	-2.371	-99.07
56(π/24)	1.0000	.8018	2.827	-2.396	-94.40	2.828	-2.397	-94.37	.7531	.6038	3.900	-2.520	-100.83	3.901	-2.522	-100.80
58(π/24)	1.0000	.8018	2.817	-2.508	-96.39	2.817	-2.509	-96.36	.7894	.6329	3.871	-2.663	-102.17	3.872	-2.665	-102.14
60(π/24)	1.0000	.8018	2.803	-2.619	-98.05	2.803	-2.620	-98.03	.8235	.6602	3.841	-2.799	-103.19	3.842	-2.801	-103.17
62(π/24)	1.0000	.8018	2.786	-2.731	-99.44	2.786	-2.732	-99.42	.8550	.6855	3.809	-2.929	-103.95	3.810	-2.931	-103.94
64(π/24)	1.0000	.8018	2.766	-2.841	-100.56	2.767	-2.842	-100.55	.8838	.7086	3.777	-3.055	-104.49	3.778	-3.056	-104.48
66(π/24)	1.0000	.8018	2.744	-2.952	-101.47	2.745	-2.953	-101.45	.9097	.7293	3.746	-3.176	-104.84	3.746	-3.178	-104.83
68(π/24)	1.0000	.8018	2.721	-3.062	-102.18	2.722	-3.063	-102.17	.9326	.7477	3.714	-3.294	-105.03	3.715	-3.296	-105.03
70(π/24)	1.0000	.8018	2.697	-3.172	-102.73	2.698	-3.173	-102.72	.9524	.7636	3.683	-3.409	-105.10	3.684	-3.411	-105.09
72(π/24)	1.0000	.8018	2.672	-3.281	-103.14	2.672	-3.283	-103.14	.9690	.7769	3.653	-3.522	-105.05	3.654	-3.524	-105.04
74(π/24)	1.0000	.8018	2.646	-3.391	-103.45	2.647	-3.392	-103.44	.9822	.7875	3.623	-3.633	-104.91	3.624	-3.635	-104.91
76(π/24)	1.0000	.8018	2.620	-3.500	-103.66	2.620	-3.501	-103.66	.9919	.7953	3.594	-3.744	-104.71	3.595	-3.746	-104.72
78(π/24)	1.0000	.8018	2.593	-3.609	-103.81	2.594	-3.611	-103.79	.9979	.8001	3.565	-3.853	-104.49	3.566	-3.855	-104.49
80(π/24)	1.0000	.8018	2.566	-3.719	-103.90	2.567	-3.720	-103.90	1.0000	.8018	3.537	-3.962	-104.28	3.538	-3.964	-104.30
82(π/24)	1.0000	.8018	2.539	-3.828	-103.97	2.540	-3.829	-103.97	1.0000	.8018	3.510	-4.071	-104.18	3.510	-4.073	-104.19

2390

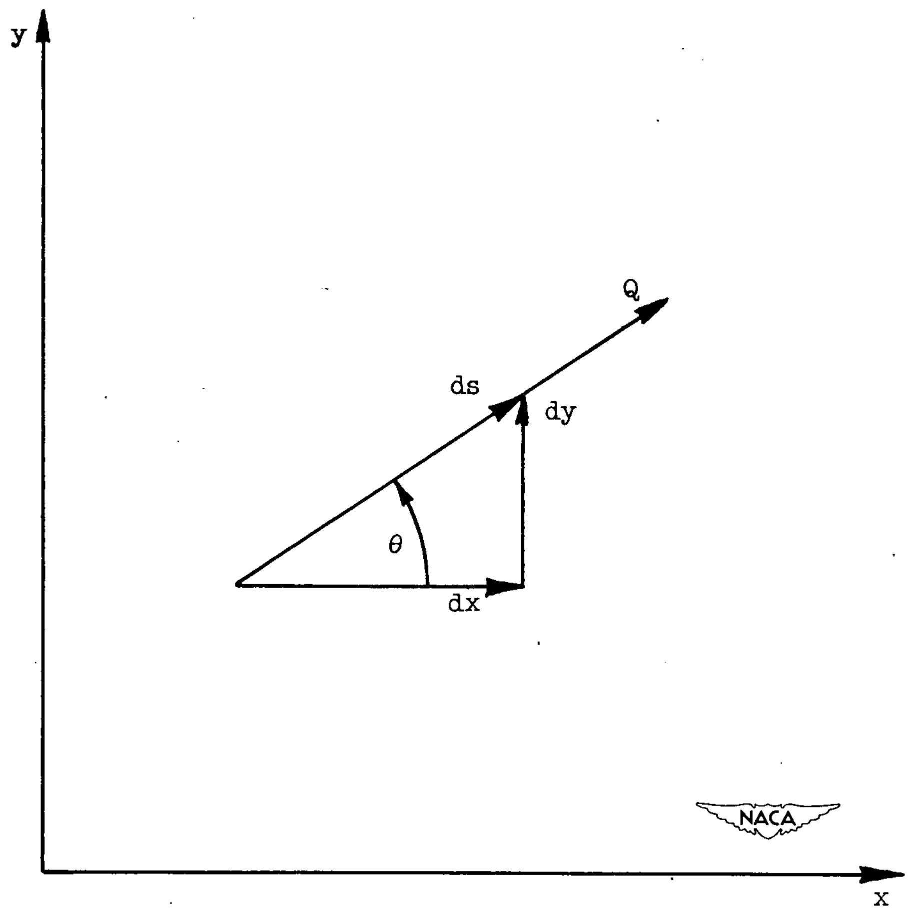

Figure 1. - Magnitude and direction of velocity at point in xy-plane.

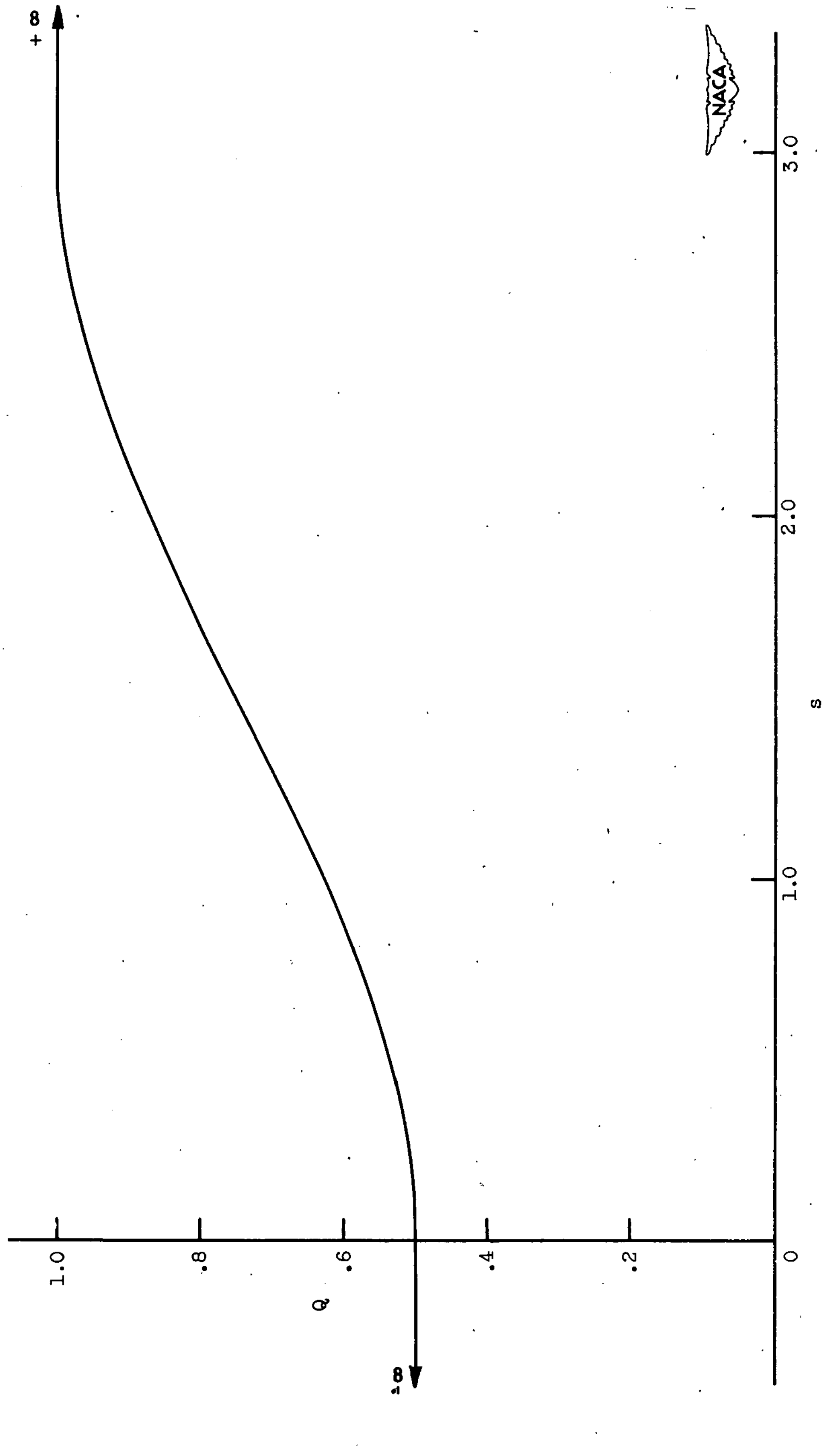

Figure 2. - Prescribed velocity distribution as function of arc length along channel wall (equation (19)).

2390

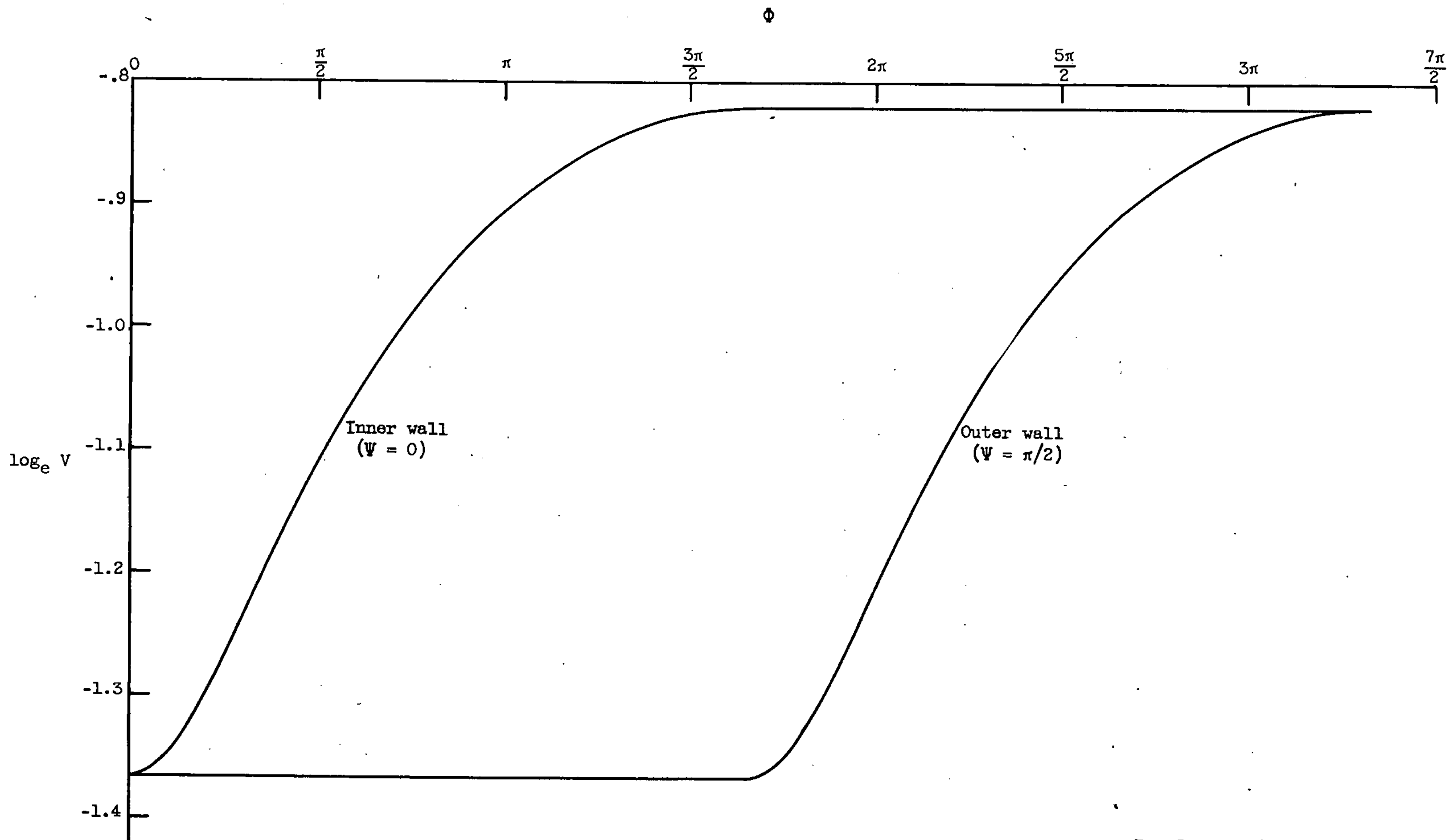

Figure 3. - Variation in prescribed values of $\log_e V$ with Φ along channel walls of numerical example.

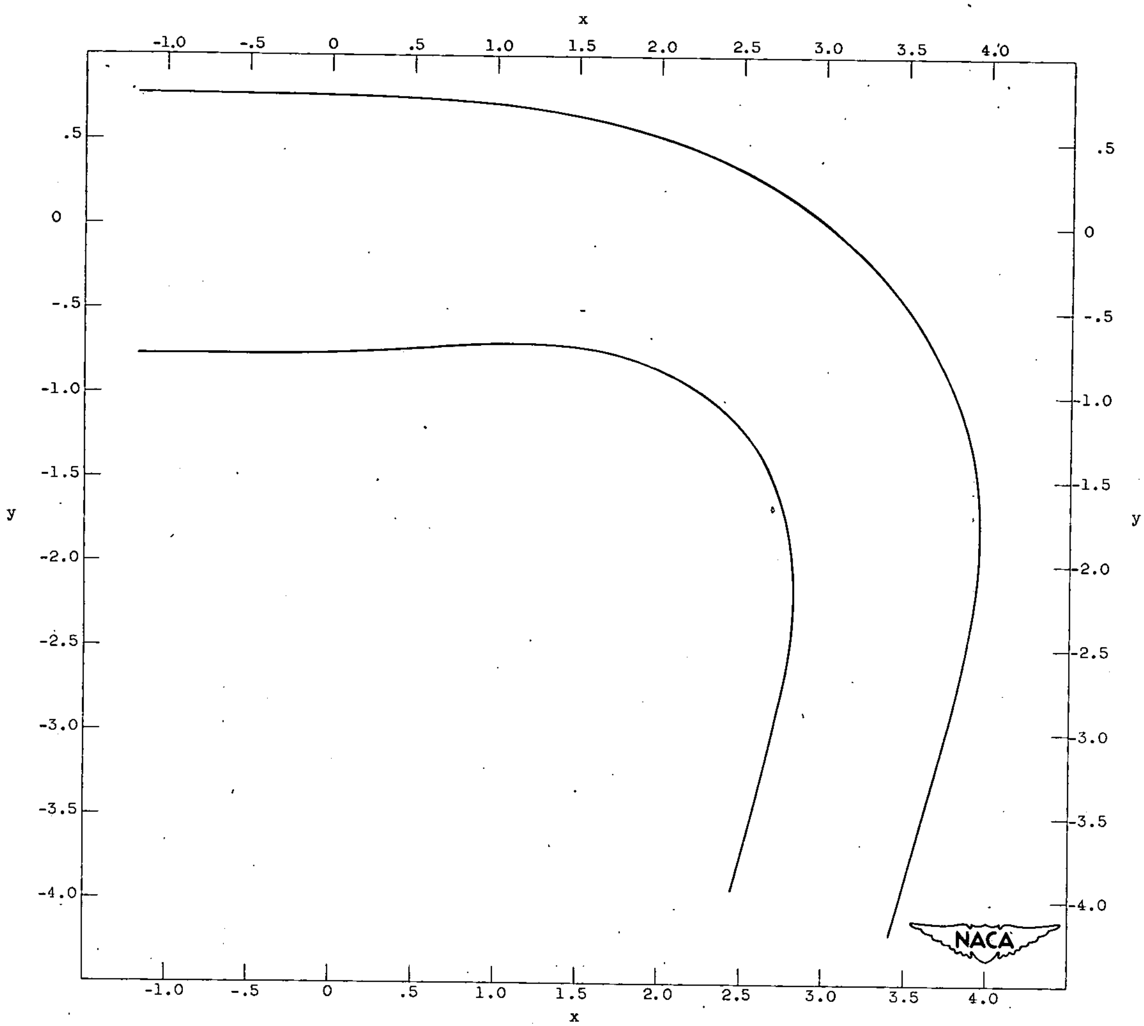

Figure 4. - Elbow design for prescribed velocity along channel walls given in figures 2 and 3.

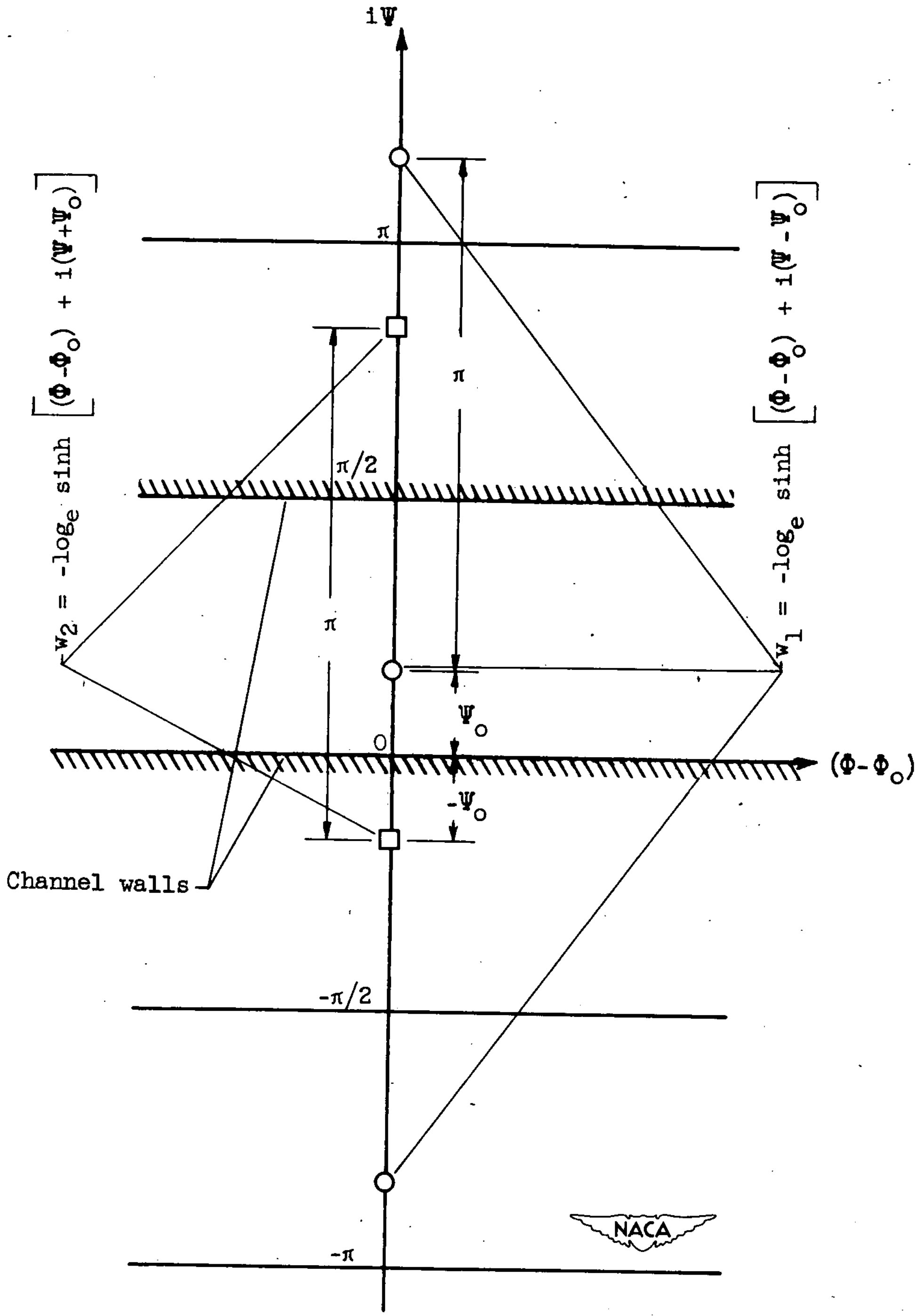

Figure 5. - Two infinite series of point sinks required in the development of Green's function of the second kind G.